RSC Advances

ROYAL SOCIETY OF CHEMISTRY

www.rsc.org/advances

Journal Name

ARTICLE

Facile Fabrication Hybrids of TiO_2@ZnO Tubes with Enhanced Photocatalytic Properties

Received 00th January 20xx,
Accepted 00th January 20xx

DOI: 10.1039/x0xx00000x

www.rsc.org/

Minghui Wang, [a] Liying Cui, [a] Songyang Li, [a] Zhuoxin Li, [a] Tianliang Ma, [a] Guoyou Luan, [a]* Wei Liu, [b] Fanli Zhang, [a]

Hollow nano-tubes of TiO_2 and TiO_2@ZnO hybrids were firstly produced by a facile and mild approach conbinning with electrospinning technique and soaking method following with the calcination. During the systhisized process, the electrospinning procedure provides the templetes for the fabrication of hollow nano-tubes by producing the PS fibres, which are in the status of porous and offer the facility for the amorphous TiO_2 immobilization through soaking method. After that, the composite fibers of TiO_2/PS and TiO_2@ZnO/PS would be calcinated into pure TiO_2 and TiO_2@ZnO tubes after complete combustion of organic materials. And then, the samples were characterized by Scanning Electron Microscopy (SEM), Transmission Electron Microscopy (TEM) and X-ray Diffraction (XRD). Ultimately, the photocatalytic performance of hybrids were evaluated from the degradation of methylene blue (MB), which exhibted an excellent photocatalytic activity. And the proposed mechnism for the enhanced photocatalytic efficiency of samples was explained at the end of paper. In principle, the approach of TiO_2 tubes fabrication is demonstrated as an effective and robust strategy to fabricate long and uniform metal-oxide micro-nano tubes in the large scale.

Introduction

As for the development of industrialization, the environment problems increased, which has made a negative influence for the health of human beings. Especially in the aspect of water pollution, a variety of contaminants have been discharged into environment, which threatens the stability of ecosystem severely.[1] Therefore, there were series of strategies which had been resorted to reduce the pollutants, such as physisorption and biological methods.[2-4] However, such methods might leave secondary waste problems. Photocatalytic oxidation as an efficient avenue for removing the contaminates of sewage water has attracted a great deal of attention.[5-7] Relative to the remediation for the water pollution, the procedure of photocatalysis is based on the advanced oxidative process, which could generate the free radical species, such as $\cdot OH$, O_2^- groups and these radicals would oxidize contaminates into small molecules, such as H_2O and CO_2 in the bulk solutions or interfacial surface of photocatalysts.[8-11]

In recent years, a number of research groups have made great effort to study the photocatalytic processes and fabrication of photocatalysts with unique nano-structures,[9] because the corresponding photocatalytic activity depends on the surface area, crystalline size, particle shape, crystalline structure, surface hydroxyl groups and other factors.[12-18] Titanium dioxide (TiO_2) has been looked as excellent candidate for photocatalytic degradation of water pollutants though the wide band gap, because photoexcitation of electron-hole pairs in surface of TiO_2 could sensitize and catalyze the UV/Visible light-induced redox procedure.[19, 20] Although enormous progresses have been achieved for enhancing the photocatalytic activity of TiO_2, the recombination of photo-generated electron-holes is still the main problem, which greatly obstructs its applications.[21] It is well known that the recombination is responsible for the low quantum yields and numerous studies confirmed that the photoelectron trapping had been regarded as an effective approach to decrease the recombination rate of charge carriers on the interior of TiO_2. Generally, the electron-traps capture the photo-induced charge carriers, which promotes the interfacial charge-transfer processes.[22-24] In order to realize the goal, some researchers suggested that the modifications for the surface of TiO_2 via dispersed fine particles, such as noble metals and some oxide semiconductor materials, could improve the charge transfer and reduce the recombination of charge carriers.[25-27] As the photocatalyst, ZnO also exhibits similar and even better activity compared with TiO_2 in principle.[28] Furthermore, ZnO has additional properties such as relative low cost, high reactivity, and nontoxicity which favors its applications in photocatalysis.[29] However, the band gaps of both ZnO and TiO_2 are relatively high, and both of them require a high-energy light source, such as UV light, to generate photo-generated

[a] College of Resources and Environment, Jilin Agricultural University, Changchun 130118, People's Republic of China
[b] State Key Laboratory on Integrated Optoelectronics, College of Electronic Science and Engineering, Jilin University, 2699, Qianjin Street, Changchun, 130012, People's Republic of China
*Corresponding author E-mail: 957478465@qq.com
† Footnotes relating to the title and/or authors should appear here.
Electronic Supplementary Information (ESI) available: [details of any supplementary information available should be included here]. See DOI: 10.1039/x0xx00000x

electrons and holes during the applications.[30] The semiconductor-semiconductor (S-S) hetero-junction has been confirmed as an effective strategy to enhance the photocatalytic activity for the charge-transfer and spatial separation of photo-generated charge carriers.[31]

Herein, we firstly reported a straightforward fabrication of the hybrid ZnO/TiO_2 hollow nanotubes via electrospinning technique combining with soaking process followed by calcination in a muffle furnace with program control device. Electrospinning technique provides an efficient and versatile approach to fabricate micro-fibers with porous structure, which were used as the templates for the nano-tubes.[32, 33] because of the porosity of the PS fibers, the solution of tetrabutyl titanate could easily enter the internal fibers and immobilize amorphous TiO_2 effectively. However, the challenges of high-efficiency nano-hybrids of photocatalyst still mainly remain in the construction of desirable interfacial structures, because the inappropriate structures of photocatalysts will limit the charge-transfer process of photo-generated electron-holes and then lower the photocatalytic property. Comparing to the other methods, such as electrode reaction,[34] chemical vapor deposition[35] and laser evaporation[36], the present work provides a facial process for the construction of hollow nano-tubes, which could serve the channel for the organic dyes fluid during the process of photocatalytic degradation and greatly improve the degradation efficiency via enlarging the interfacial adsorption to the methylene blue (MB). Simultaneously, the strategy of fabrication for hollow nano-tube may have huge potential for the outstanding materials after self-assembly modification in the future.

Experimental section

Materials and methods

PS and tetrabutyl titanate ($Ti(OBu)_4$ 97%) were purchased from the Sigma Aldrich and the PS with Mw=350000g/mol; N, N-dimethylformamide (DMF), Absolute methanol and Ethyl alcohol were bought from the Beijing chemical works, zinc acetate and Polyvinylpyrrolidone (PVP) used in the experiment were purchased from Aladdin. And all of chemicals used in the experiments were analytic and without further purification. The following is the synthesis process:

At first, the PS fibers were fabricated by electrospinning equipment with high voltage power supply, spinning nozzle and collector connected with the ground. The precursor of spinning solution was made up with 2.3g PS and 7.7g DMF. After complete dissolution of PS in the DMF, it was transferred into the syringe. The feeding rate of solution was controlled at 1.5 ml/h. The voltage applied to the spinning needle (Number 10) was 14.20 kV, and distance from the tip to the collector was 20 cm with the humidity of 20% in the air.

And then, the membrane was put in the solution of tetrabutyl titanate and ethyl alcohol for 2h and the volume ratio of Tetrabutyl titanate and Ethyl alcohol was 1:10. After soaking process, the composite membrane was shifted into the drying oven for one hour.

Ultimately, the TiO_2/PS fibers were immersed in the mixture of zinc acetate solution. The concentrations of Zn^{2+} were 0.01 M and 0.1 M, respectively. And the concentration of PVP was 1.2% in mass fraction, which was used as stabilizer agent for Zn^{2+}. The solvent of solution was Absolute methanol, which have a good solubility for zinc acetate.

The last step is calcination. The TiO_2/PS and TiO_2@ZnO/PS membrane was calcined at 550 ℃ for 0.5 h in the rate of 2 ℃ min^{-1} to burn the organic compound of templates of PS completely, then, the hybrids of hollow nano-tubes were fabricated.

Characterization

The samples were measured by D/MAX 2250 V diffractometer (Rigaku, Japan, XRD) to confirm the crystal phase of hybrids. The morphologies of PS and hollow-tubes were characterized via Scanning Electron Microscopy (SEM JEOL JSM-7500F) and Transmission electron microscopy (TEM JEM-2010) under a working voltage of 200 kV equipped with an energy dispersive X-ray (EDX) spectrometer. UV-vis spectra were recorded on a UV-vis spectrophotometer (UV-2550, Shimadzu) with a scanning range from 300 to 800 nm. Photoluminescence (PL) spectra were recorded by fluorescence spectrometer (Jobin Yvon Fluoro Max–4) with the excitation wavelength of 320 nm. And the degradation process was monitored by the UV-Vis spectrophotometer measuring the absorption of MB at 664 nm.

Photocatalytic tests for degradation of MB

The tests were carried out under UV illumination by a wide-band lamp bulb (125 W Philips TL/05) with a predominant wavelength of 365 nm, and the photo-reactor was an ordinary glass of 250 mL equipped with circulating water at room temperature. And the photocatalytic activities of samples were tested under visible light, which was generated by an internal 150 W high-pressure xenon lamp with UV cut-off glass filter transmitting λ >400 nm. During the degradation of process, the methylene blue (MB) was used as degradation agent to evaluate the photocatalytic activity of samples. Firstly, the four tests were put in the darkness for 2h to ensure the establishment of adsorption–desorption equilibrium between the MB dye and as-prepared tubes. An aliquot (3 mL) of the solution was taken out at half an hour intervals during the experiment and tested using a UV-vis spectrophotometer (Hitachi U-3010), and after that the analyzed aliquot would be poured back into the glass reactor immediately to ensure a roughly equivalent volume of solution. Finally, the photocatalytic activities were decided by the degradation efficiency from the data of absorbance.

Results and discussion

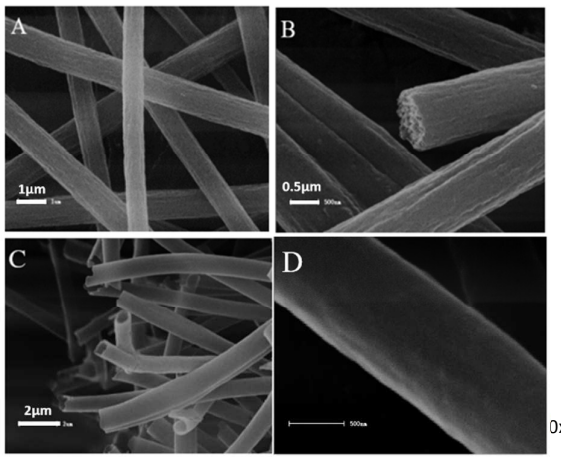

Fig. 1 The SEM images of samples (A SEM image of PS fibers; B the morphology for the cross section of PS fiber; C the low magnification of SEM image for TiO_2 tubes; D the high magnification of SEM image of TiO_2 tube)

Fig. 1 shows the typical microstructure of PS fibres and pure TiO_2 tubes. The PS fibers with the high porosity were produced by electrospinning technique and used as templates for fabrication of hollow tubes, which could provide the channel for TBOT diffusion (Fig. 1B). The scanning electron microscopy image of calcined TiO_2 nanotube reveal that the diameters of tubes was in the range of 1-1.3 μm and the thickness of the shell of tube was estimated to be 20-50 nm observed from the SEM and TEM images. Furthermore, the morphology of hybrids and pure TiO_2 tubes still maintained in good after calcination. As shown in Fig. 2A and 2B, the surface of hybrid of TiO_2@ZnO still maintain in smooth, which attributed to the shrinkage of fibres during the process of calcination. Compared with Fig. 1 and Fig. 2, there were not any difference for the morphology of fibrous surface after the addition of ZnO, which indicated that there was no obvious aggregation for the ZnO nanoparticles and the Zn^{2+} ions were distributed on the surface of fibres evenly. After soaking in the solution of Zn^{2+} ions, the TiO_2 particles would react with the zinc acetate to form the lattice type of $ZnTiO_3$ by calcination to remove organic matter at 550 ℃, which could be proofed from the crystal phase in the Fig. 3.[37] Importantly, the outer wall of hollow tube could be tuned by varying the concentration of Tetrabutyl Titanate (TBOT) and electrospinning parameters, because the diameter of tubes was ascribed to the diameter of electrospinning fibres. Generally, electrospinning technique is a versatile approach for generating the fibers with specific structures via adjusting the concentrations of polymer, conductivity and surface tension of solutions.

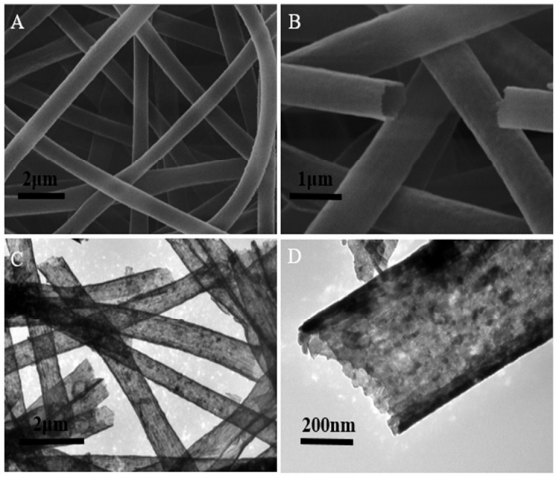

Fig. 2 The SEM and TEM images of samples (A SEM image of pure TiO_2@ZnO tubes; B the SEM image of cross section for TiO_2@ZnO; C TEM image of TiO_2@ZnO and D the high magnification of TiO_2@ZnO TEM image)

To further investigate the interior crystal structure, XRD was used to measure the phases of TiO_2@ZnO hybrids and pure TiO_2 tubes. And the EDX spectrum were used to confirm the composition of samples after calcination. As we can see from Fig. 1S, the organic matters had been burned completely. The Fig. 3 shows the XRD spectra of pure tube of TiO_2 and hybrid of TiO_2@ZnO calcined at 550 ℃ for 0.5 h with the heating rate of. 2 ℃/min. The green curve in Fig. 3 represents the XRD pattern of pure TiO_2 tubes, and the XRD patterns match their JCPDS files No # 21-1272, which corresponds to the anatase in the phase. However, there is a certain amount of rutile phase in the pure TiO_2 tubes. In comparison with diffraction profiles of TiO_2@ZnO hybrids, the peaks of $ZnTiO_3$ (JCPDS No # 26-1500) have been enhanced gradually with the increase of ZnO. In the case of hollow nano-tubes, the XRD patterns of all three samples have shown the rutile peak in the 2θ=27.4°, however, the peak intensity was substantially decreased due to the addition of metal ions of Zn^{2+}, which could impede the transition for TiO_2 from anatase to rutile. [38]

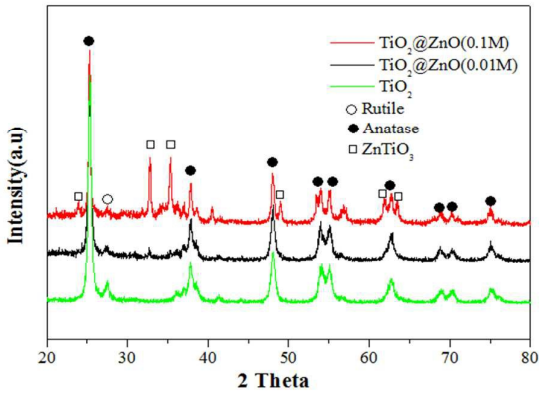

Fig. 3 The XRD patterns of the as-synthesized products

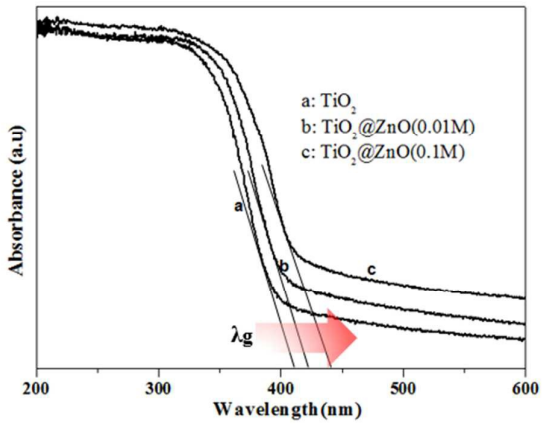

Fig. 4 UV-vis DRS of TiO_2 tubes, TiO_2@ZnO (0.01M) and TiO_2@ZnO (0.1M)

As the photocatalysts, the photocatalytic efficiency of TiO_2@ZnO hollow tubes is closely related to the light

absorption amount and wavelength range. The UV-Vis DRS is an effective measurement for detecting the interfacial properties of photocatalysts, which could provide references for the photo-oxidation performance of the materials. As observed from the Fig. 4, the absorption spectra of samples are depicted. The UV-Vis adsorption spectrum indicated that the TiO_2@ZnO (0.1M) had a broad absorption from the range of 350-600nm, especially in the absorption for the visible light compared with pure TiO_2 tubes, which demonstrated that the hybrids need lower energy than pure TiO_2 tubes to be excited. The absorption edges of samples appear at 409, 420 and 442nm for the TiO_2, TiO_2@ZnO (0.01 M) and TiO_2@ZnO (0.1 M), respectively. With the addition of ZnO, the absorption intensity for the UV and visible light has been enhanced. Furthermore, there is significant red-shift with lower band energy of TiO_2@ZnO hybrids comparing with the TiO_2 tubes. Therefore, the results indicated that the hollow tubes of TiO_2@ZnO could absorb lights in the visible range, and the lights could be utilized more efficiently for the photocatalytic purpose. Simultaneously, as suggested by XRD patterns, the $ZnTiO_3$ crystallites have been formed in the hybrids, thus, it might induce defects to the crystal lattice structure of TiO_2 or ZnO, leading to an increasing of absorption edge.

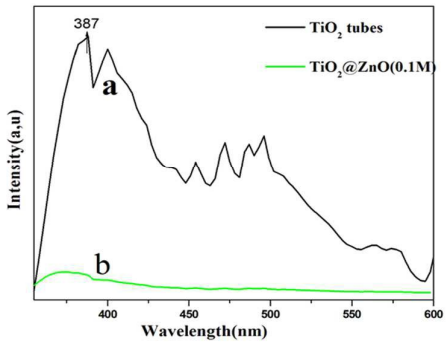

Fig. 5 Photoluminescence (PL) spectra of (a)TiO_2 and (b) TiO_2@ZnO (0.1 M) λ_{EX} = 320 nm

PL spectra is related to the transfer behaviour of photo-generated electrons and holes, therefore, the PL spectra could reflect the separation and recombination of charge carriers. As we can see from the Fig. 5, the PL spectra of TiO_2 tubes have a strong emission peak at 387 nm with the excitation wavelength at 320 nm, however, the PL intensity of hybrid decreased greatly with the addition of ZnO.[39] The most important reason for the phenomenon is the defects of crystal structure of TiO_2, which would act as traps for capturing the photo-excited electrons, and thus inhibit recombination of e^- /h^+ pairs. The PL spectrum results are consistent with the photocatalytic activity of TiO_2 tubes and TiO_2@ZnO hybrids under UV and visible light.

Owing to the absorption peaks of MB in the visible range, therefore, its degradation rate can be easily monitored with UV-vis spectrophotometer. Moreover, the MB is poorly biodegradable and main contaminant in wastewater, which is the large portion of textile dye and industrial dyes stuffs. Therefore, in order to evaluate the photocatalytic property of theTiO_2@ZnO hollow tubes, MB was used as a test contaminant during the degradation process under UV illumination. For comparison, four photocatalytic degradation tests were carried out for decomposition of MB dyes in the solution with hybrids and pure TiO_2 tubes as photocatalyst, darkness without photocatalyst and blank test, respectively. As observed from the photocatalytic degradation curves, the hybrids of TiO_2@ZnO decolorized MB faster than the pure TiO_2 hollow tubes and after three hours UV irradiation, the degradation efficiency for MB were 95.27% and 83.25%. In order to investigate the stability of the hybrids of TiO_2@ZnO tubes, the sample was repeatedly used for four times after separation via centrifugation and drying. The photocatalytic degradation efficiency was evaluated by E_c/E_0 (E_c was the degradation efficiency of reuse time and E_0 was the first time degradation efficiency). Regretfully, the photocatalytic activity of TiO_2@ZnO reduced obviously after second repeated use under UV irradiation. To find the above reason, we examined the morphology of sample after second repeated use. As shown from Fig. S2, the structure of hybrid TiO_2@ZnO had been destroyed, therefore, it would make some influence for the photocatalytic performance. Additionally, the loss of small amount of sample in process of recycle would also lower the photocatalytic efficiency than before. The detailed plots of degradation efficiency for MB dyes were shown in the Fig. 6. Interestingly, the intensity of the maximum absorption peaks of MB have a distinct blue-shifted with the photo-degradation continued, especially for that of TiO_2@ZnO as revealed in the Fig. 6. This is because the formation of the demethylated dyes during the process of degradation, which would lead to the multicomponent system and blue-shift.[40] Furthermore, the hybrid as catalyst exhibited higher efficiency than that of pure TiO_2 for degradation of MB under visible light in same conditions. The degradation efficiency of TiO_2@ZnO for MB reached to 36.52%, whereas, the TiO_2 tubes' degradation for MB was just about 24.54%. Therefore, the hybrids exhibited better photocatalytic activity than that of pure TiO_2 tubes. So, the fabrication of TiO_2@ZnO provided a

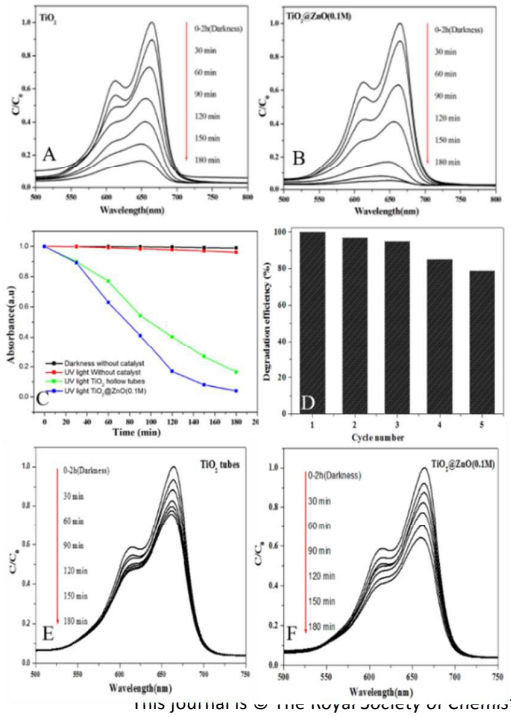

new way to enhance the photocatalytic activity.

Fig. 6 Photocatalytic degradation of MB in the presence of TiO_2 tubes, TiO_2@ZnO hybrids (A-D were degradation curves of samples and degradation efficiency under UV light, E and F were degradation efficiency of TiO_2 tubes and TiO_2@ZnO (0.1 M) respectively)

Compared with the degradation efficiency of two samples, the TiO_2@ZnO nanotubes exhibited higher photocatalytic efficiency under UV light, which was consistent with the results of UV-Vis DRS. As for the hybrids of TiO_2@ZnO, the enhanced photocatalytic activity
for decomposing MB dye could be ascribed to the certain amount of ZnO.[41] On the surface of TiO_2 hollow tubes, there are some zinc oxide particles distributed uniformly, which would form a semiconductor-semiconductor (S-S) heterostructure with TiO_2.[31] Fig. 7 is the schematic of photocatalytic mechanism. In principle, the ZnO could be regarded as the modification for the surface of TiO_2 tubes, which belongs to the type Ⅱ semiconductor hetero-junction.[42] When the hybrids of TiO_2@ZnO are excited under UV illumination with higher energy photons than the band gap, there would be a great deal of electrons promoted from valence band (VB) to the conduction band (CB) of ZnO and TiO_2, respectively.[43] Then, the electrons would be transferred from CB of ZnO to CB of TiO_2. Additionally, the photo-generated holes existed in the VB of TiO_2 are transferred to the VB of ZnO. After two of transfer of electrons and holes, the photo-generated electron/hole could be effectively separated, therefore, the recombination rate of the electron–hole pair should be decreased in some degree.[44] Simultaneously, the electrons and holes, located in the CB of TiO_2 and VB of ZnO, respectively, would react with O_2 and H_2O to produce the radical species, such as $OH\cdot$, HO^-_2 and O^-_2. These radical species would oxide the organic dyes absorbed on the surface of photocatalyst directly.[45] Except that the hetero-junction effect improves the photocatalytic activity, the special structure of hybrids could also promote the photocatalytic process for the hollow structures, which have provided a channel for the dyes distribution and enlarged the interfacial surface area with bulk solutions. Thus, the redox process has been enhanced vastly.

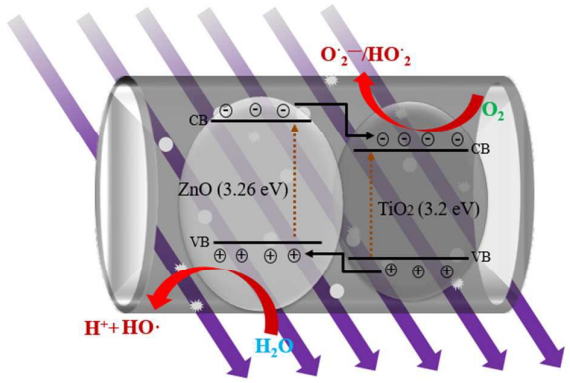

Fig. 7 The schematic of electron-hole separations and energy band matching of TiO_2@ZnO heterostructures under UV illumination

Conclusions

In summary, the facile fabrication procedure was demonstrated to prepare the hollow nano-tube of TiO_2@ZnO hybrids effectively. And during the preparation process, the electrospinning technique provides an effective approach to generate the micro-nano fibres, which serve as the templates for the fabrication of micro-tubes. Furthermore, the hybrids of TiO_2@ZnO exhibited excellent photocatalytic activity in the degradation of MB dyes compared with pure TiO_2 tubes. The most significant is the methodology, which furnished a new avenue for preparation the hollow nano-tubes or core-shell materials in the relatively mild and environmental benign approach. Therefore, it possesses great potential for the applications of various fields in the future.

Acknowledgement

M. H. Wang thanks to the financial support of the Doctor funding (No. 201218).

References

1. C. J. Vörösmarty, P. B. McIntyre, M. O. Gessner, D. Dudgeon, A. Prusevich, P. Green, P. M. Davies, *Nature*, 2010, **467**, 555.
2. M. Rafatullah, O. Sulaiman, R. Hashim, A. Ahmad, *Journal of hazardous materials,* 2010 **177**, 70.
3. A. Ahmad, S. Hamidah Mohd-Setapar, C. Sing Chuong, A. Khatoon, W. A. Wani, R. Kumar and M. Rafatullah, *RSC Adv.*, 2015, **5**, 30801.
4. K. C. Kemp, H. Seema, M. Saleh, N. H. Le, K. Mahesh, V. Chandra, K. S. Kim, *Nanoscale,* 2013, **5**, 3149.
5. S. Vadahanambi, S. H. Lee, W. J. Kim, I. K. Oh, *Environmental science & technology*, 2013, **47,** 10510.
6. V. Corcé, L. M. Chamoreau, E. Derat, J. P. Goddard, C. Ollivier, L. Fensterbank, *Angewandte Chemie*, 2015, **127**, 11576.
7. A. Di Paola, M. Bellardita, B. Megna, F. Parrino, L. Palmisano, *Catalysis Today,* 2015, **252**, 195.
8. L. Ismail, A. Rifai, C. Ferronato, L. Fine, F. Jaber, J. M. Chovelon, *Applied Catalysis B: Environmental*, 2016, **185**, 88.
9. Q. Sun, K. Lv, Z. Zhang, M. Li, B. Li, *Applied Catalysis B: Environmental*, 2015, **164**, 420.
10. T. P. Yoon, M. A.Ischay, J. Du, *Nature Chemistry,* 2010, **2**, 527.
11. L. Zhou, W. Wang, H. Xu, S. Sun, M. Shang, *Chemistry–A European Journal*, 2009, **15**, 1776.
12. S. Girish Kumar and K. S. R. Koteswara Rao, *RSC Adv.*, 2015, **5**, 3306.
13. Y. Liu, J. Goebl and Y. Yin, *Chem. Soc. Rev.*, 2013, **42**, 2610.
14. A. Kar and A. Patra, *J. Mater. Chem. C*, 2014, **2**, 6706.
15. A. Primo, A. Corma and H. García, *Phys. Chem. Chem. Phys.*, 2011, **13,** 886.
16. M. Wang, J. Ioccozia, L. Sun, C. Lin and Z. Lin, *Energy Environ. Sci.,* 2014, **7**, 2182.
17. P. Kar, S. Sardar, S. Ghosh, M. R. Parida, B. Liu, O. F. Mohammed, P. Lemmens and S. K. Pal, *J. Mater. Chem. C,* 2015, **3**, 8200.
18. W. Ong, L. Tan, S. Chai, S. Yong and A. Mohamed, *Nanoscale*, 2014, **6**, 1946.
19. Y. Zhang, Z. Jiang, J. Huang, L. Y. Lim, W. Li, J. Deng, D. Gong, Y. Tang, Y. Lai and Z. Chen, *RSC Adv.,* 2015, **5,** 79479.

20. D. María Hernández-Alonso, F. Fresno, S. Suárez and J. M. Coronado, *Energy Environ. Sci.,* 2009, **2**, 1231.
21. W. Zhou, H. Liu, J. Wang, D. Liu, G. Du, J. Cui, *ACS applied materials & interfaces*, 2010, **2**, 2385.
22. Y. Hou, X., Li, Q. Zhao, X. Quan, G. Chen, *Journal of Materials Chemistry*, 2011, **21**, 18067.
23. J. Xiao, Y. Xie, H. Cao, F. Nawaz, S. Zhang, Y. Wang, *Journal of Photochemistry and Photobiology A: Chemistry, 2016,* **315***,* 59.
24. S. G. Kumar, L. G. Devi, T*he Journal of Physical Chemistry A*, 2011, **115**, 13211.
25. W. Zhao, W. Ma, C. Chen, J. Zhao, Z. Shuai, Journal of the American Chemical Society, 2004, **126**, 4782.
26. F. Zhang, Z. Cheng, L. Kang, L. Cui, W. Liu, G. Hou, H. Yang and X. Xu, *RSC Adv.*, 2014, **4**, 63520.
27. A. Bumajdad and M. Madkour, *Phys. Chem. Chem. Phys*., 2014, **16**, 7146.
28. F. Lu, W. Cai, Y. Zhang, *Advanced Functional Materials*, 2008, **18**, 1047.
29. S. Malato, P. Fernández-Ibáñez, M. I. Maldonado, J. Blanco, W. Gernjak, *Catalysis Today*, 2009, **147**, 1.
30. S. Girish Kumar and K. S. R. Koteswara Rao, *RSC Adv.*, 2015, **5**, 3306.
31. C. Cheng, A. Amini, C. Zhu, Z. Xu, H. Song, N. Wang, *Scientific reports, 2014,* ***4***.
32. J. Lin, B., Ding, J. Yu, *ACS applied materials & interfaces*, 2010, **2**, 521.
33. W. Liu, C. Huang, X. Jin, *Nanoscale research letters*, 2014, **9**, 1.
34. Y. C. Nah, A. Ghicov, D. Kim, S. Berger, P. Schmuki, Journal of the American Chemical Society, 2008, **130**, 16154.
35. J. W. Do, D. Estrada, X. Xie, N. N. Chang, J. Mallek, G. S. Girolami, J. W. Lyding, *Nano letters*, 2013, **13**, 5844.
36. A. Bjelajac, R. Petrovic, G. Socol, I. N. Mihailescu, M. Enculescu, V. Grumezescu, D. Janackovic, *Ceramics International*, 2016, **42**, 9011.
37. M. H. Hossein, M. Mikhak, *Current Nanoscience*, 2011, **7**, 603.
38. K. Wilke, H. D. Breuer, *Journal of Photochemistry and Photobiology A: Chemistry,* 1999, **121**, 49.
39. L. Jing., Y. Qu., B. Wang., S. Li., B. Jiang, L. Yang, W. Fu, H. Fu, J. Su. *Solar Energy Materials and Solar Cells*, 2006, **90**, 1773.
40. R. Ullah, *J. Dutta, Journal of hazardous materials,* 2008, **156**, 194.
41. Z. Zhang, Y. Yuan, Y. Fang, L. Liang, H. Ding, L. Jin, *Talanta*, 2007, **73**, 523.
42. K. Shen, K. Wu, & D. Wang, *Materials Research Bulletin*, 2014, **51**, 141.
43. R. Liu, H. Ye, X. Xiong, H. Liu, *Materials Chemistry and Physics*, 2010, **121**, 432.
44. D. L. Liao, C. A. Badour, B. Q. Liao, *Journal of Photochemistry and Photobiology A: Chemistry*, 2008, 194, **11**.
45. A. Adel Ismail and W. Bahnemann, Detlef, *J. Mater. Chem.,* 2011, **21**, 11686.

Graphic abstract

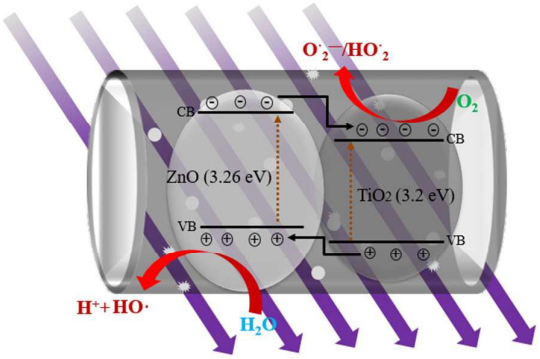

The schematic of electron-hole separations and energy band matching of TiO_2@ZnO heterostructures under UV illumination